Progress In Electromagnetics Research, Vol. 115, 409–422, 2011

DRIVING A DIELECTRIC CYLINDRICAL PARTICLE WITH A ONE DIMENSIONAL AIRY BEAM: A RIGOROUS FULL WAVE SOLUTION

W. Lu, J. Chen, and Z. Lin

State Key Laboratory of Surface Physics and Department of Physics
Fudan University, Shanghai 200433, China

S. Liu

Institute of Information Optics
Zhejiang Normal University, Jinhua, Zhejiang 321004, China

Abstract—We present a rigorous full wave calculation of the optical force on a dielectric cylindrical particle of an arbitrary size under the illumination of one dimensional (1D) Airy beam. The radiation force is written in terms of the cylindrical partial wave expansion coefficients of the non-paraxial 1D Airy beams. Our simulation results demonstrate that an Airy beam can accelerate the microparticles along its parabolic trajectory, while transverse to which the particles are trapped at the center of its main lobe, corroborating the possibility of the long distance particle transport by means of an Airy beam.

1. INTRODUCTION

Airy beams, inspired by the nonspreading Airy wave packet solution in the context of quantum mechanics [1, 2], was first successfully generated using phase-modulated Gaussian beam in 2007 [3, 4], decades after the proposal of its theoretical quantum mechanics analogue. In contrast to other non-diffracting beams such as Bessel beams [5, 6] and Mathieu beams [7], resulting from an appropriate conical superposition of plane waves [8, 9] and showing non-spreading characteristics along straight trajectories, Airy beams remain quasi-diffraction-free over long distance while their main lobes accelerate during propagation along parabolic trajectories. As Airy beams do not originate from the conical superposition of plane waves, they are realizable even

Received 17 March 2011, Accepted 11 April 2011, Scheduled 12 April 2011
Corresponding author: Wanli Lu (082019042@fudan.edu.cn).

in one-dimension [4]. The unique features of Airy beams enable many applications, which, amongst others, include novel optical micromanipulation such as "optically mediated particle clearing" [10].

Pioneered by Ashkin [11, 12], optical micromanipulation based on optical force has become a substantial field that has a major impact on a variety of disciplines ranging from the microscopic to atomic scales [13–15]. Microparticles can be guided to follow trajectories incommensurate with the flow direction of fluid with the help of the gradient and scattering forces originated from light beams. The use of exotic light beams, in addition to Gaussian beams, has come into prominence for the optical micromanipulation in biological and colloidal sciences [10, 16, 17]. For instance, the "nondiffracting" Bessel beams have been employed to trap microscopic particles in multiple planes [16]. Trapping by optical vortices, namely, by beams that carry optical angular momentum, may exhibit supercritical Andronov-Hopf bifurcation [17]. In particular, the quasi-diffraction-free Airy beams have also been used in achieving highly robust and efficient optical manipulation termed "optically mediated particle clearing" [10]. However, there appears no theoretical analysis of the optical force experienced by microparticles in the Airy beam field. In this paper, we present a rigorous full wave calculation of the optical force exerted on a two-dimensional (2D) particle of arbitrary size by Airy beams. The results presented are expected to be applicable to the optical micromanipulation of micro-rods with finite length using one dimensional Airy beams, provided that their lengths are much greater than the diameters.

2. DESCRIPTION OF AN AIRY BEAM

An incident Airy beam propagating along x-axis with its electric field polarized along z-axis is considered in 2D case. The configuration is shown in Fig. 1 where the input plane of the system is set to be $x = 0$. The initial field profile is [3, 4, 18–20]

$$E_z(x = 0, y) = E_0 \mathrm{Ai}(y/y_0) \exp(\alpha y/y_0), \tag{1}$$

where $\alpha > 0$ is the parameter measuring the power conveyed by beams, y_0 is the transverse scale, and $E_0 \mathrm{Ai}(\Delta y/y_0) \exp(\alpha \Delta y/y_0)$ with $\Delta y = -0.937173 y_0$ is the amplitude in the center of the main lobe. As α becomes smaller, the Airy beam with finite power tends to be a real non-diffraction beam. For the case when $\alpha = 0$, it becomes a non-spreading wave packet discussed firstly by Berry and Balazs [1] in 1978. With the increase of the transverse scale y_0, the spatial width of the main lobe [4] becomes larger and larger. In the paper, the time harmonic factor $\exp(-i\omega t)$ is assumed and suppressed.

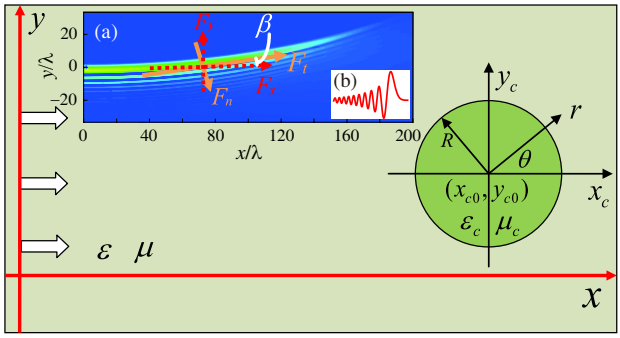

Figure 1. The schematic diagram of an incident Airy beam interacting with a dielectric circular cylinder. R and (x_{c0}, y_{c0}) are the radius and the center of the cylinder, respectively. The origin of the coordinates system x_c-o_c-y_c is chosen to be located at the center of the cylinder. The inset (a) shows the intensity distribution of the incident Airy beam propagating along x-axis. And the inset (b) is the initial field profile along y-axis in the plane $x = 0$.

Based on the plane wave spectrum representation [21, 22], an Airy beam can be written in Cartesian vector components as

$$E_z(x, y) = \int_{-\infty}^{\infty} c_z(p, q) \exp\left[ik(px + qy)\right] \mathrm{d}q, \tag{2}$$

where k is the wavenumber in the background medium, (p, q) is the propagation direction of the component plane wave ($p = \cos\gamma$, $q = \sin\gamma$, with γ the propagation angle of the plane wave), and $c_z(p, q)$ is the complex amplitude of the plane wave, determined by the field profile in the initial plane $x = 0$. It can be obtained from the following inverse Fourier transform

$$\begin{aligned} c_z(p, q) &= \frac{1}{\lambda} \int_{-\infty}^{\infty} E_z(x = 0, y) \exp\left[-ik(px + qy)\right] \mathrm{d}y \\ &= E_0 \frac{y_0}{\lambda} \exp\left[(\alpha - iky_0q)^3/3\right], \end{aligned} \tag{3}$$

where λ is the wavelength of the Airy beam in the background medium. A useful relation can be found in P55 in [23] to calculate the above angular spectrum. With these knowledge, the field profile at an arbitrary point can be obtained from Eq. (2).

We then focus on the Cartesian coordinate system x_c-o_c-y_c for the circular shape boundary, and its corresponding cylindrical coordinate is (r, θ), i.e., $x_c = r\cos\theta$, $y_c = r\sin\theta$. Since there is no rotation between two Cartesian coordinate systems (shown in Fig. 1), so the

transformation between them are $x = x_c + x_{c0}$ and $y = y_c + y_{c0}$. Accordingly, the term $\exp[ik(px+qy)]$ in Eq. (2) can be written in the form [24] below in the coordinate system x_c-o_c-y_c as

$$\begin{aligned}\exp[ik(px+qy)] &= \exp[ik(px_{c0}+qy_{c0})]\exp[ik(px_c+qy_c)] \\ &= \exp[ik(px_{c0}+qy_{c0})]\sum_{n=-\infty}^{\infty} i^n J_n(kr)\exp[in(\theta-\gamma)], \end{aligned} \tag{4}$$

where we have used the following relation

$$\begin{aligned}\exp(i\mathbf{k}\cdot\mathbf{r}) &= \exp[ikr(p\cos\theta+q\sin\theta)] \\ &= \sum_{n=-\infty}^{\infty} i^n J_n(kr)\exp[in(\theta-\gamma)], \end{aligned} \tag{5}$$

with $J_n(kr)$ the Bessel function of order n. Then we get the field profile of a non-paraxial Airy beam at an arbitrary point described in the cylindrical coordinates

$$\begin{aligned}E_z(r,\theta) &= \int_{-\infty}^{\infty}\frac{y_0}{\lambda}\exp\left[(\alpha-iky_0q)^3/3\right]\exp[ik(px_{c0}+qy_{c0})] \\ &\quad\times\sum_{n=-\infty}^{\infty} E_0 i^n J_n(kr)\exp[in(\theta-\gamma)]\,\mathrm{d}q, \end{aligned} \tag{6}$$

where the term $\sum i^n J_n(kr)\exp(in\theta)$ is independent on q, and can be extracted from the integral. For convenience, we set

$$\begin{aligned}p_{1n} &= \int_{-\infty}^{\infty}\frac{y_0}{\lambda}\exp\left[(\alpha-iky_0q)^3/3\right]\exp[ik(px_{c0}+qy_{c0})] \\ &\quad\times\exp(-in\gamma)\mathrm{d}q. \end{aligned} \tag{7}$$

In this manner, the incident Airy beam can be expanded into cylindrical waves in the form

$$E_z(r,\theta) = \sum_{n=-\infty}^{\infty} E_0 i^n p_{1n} J_n(kr)\exp(in\theta). \tag{8}$$

To make Eq. (8) applicable in realistic situation, we have to evaluate the expansion coefficients p_{1n} of the incident Airy beam numerically. The integrand in Eq. (7) is highly oscillatory, adding considerably to the difficulty of numerical calculation. It follows from Eq. (7) that $\exp(-in\gamma) = (p-iq)^n$, with $p = \sqrt{1-q^2}$ for the case when $(q^2 \le 1)$ and $p = i\sqrt{q^2-1}$ for the case when $(q^2 > 1)$. Then, with a simple mathematical manipulation Eq. (7) is decomposed into,

$$p_{1n} = c_n^{(1)} + c_n^{(2a)} + c_n^{(2b)}, \tag{9}$$

where

$$\begin{aligned} c_n^{(1)} &= \int_{-\infty}^{0} \frac{y_0}{\lambda} \exp\left[(\alpha - iky_0q)^3/3\right] \exp[ik(px_{c0} + qy_{c0})](p - iq)^n \mathrm{d}q, \\ c_n^{(2a)} &= \int_{0}^{1} \frac{y_0}{\lambda} \exp\left[(\alpha - iky_0q)^3/3\right] \exp[ik(px_{c0} + qy_{c0})](p - iq)^n \mathrm{d}q, \\ c_n^{(2b)} &= \int_{1}^{+\infty} \frac{y_0}{\lambda} \exp\left[(\alpha - iky_0q)^3/3\right] \exp[ik(px_{c0} + qy_{c0})](p - iq)^n \mathrm{d}q. \end{aligned} \tag{10}$$

The integrand in Eq. (10) can be regarded as functions of complex variable z given by

$$\begin{aligned} f(n,z) =& \frac{y_0}{\lambda} \left(\sqrt{1-z^2} - iz\right)^n \exp\left[(\alpha - iky_0z)^3/3\right] \\ & \times \exp\left[ik\left(\sqrt{1-z^2}x_{c0} + zy_{c0}\right)\right], \end{aligned} \tag{11}$$

$$\begin{aligned} g(n,z) =& \frac{y_0}{\lambda} \left(-\sqrt{1-z^2} - iz\right)^n \exp\left[(\alpha - iky_0z)^3/3\right] \\ & \times \exp\left[ik\left(-\sqrt{1-z^2}x_{c0} + zy_{c0}\right)\right]. \end{aligned} \tag{12}$$

With the contours shown in Fig. 2, it is easy to arrive at

$$\begin{aligned} c_n^{(1)} &= -\int_{C_-} f(n,z)\mathrm{d}z = -\int_{\widetilde{C}_-} f(n,z)\mathrm{d}z, \\ c_n^{(2a)} &= \int_{\widetilde{C}_+} f(n,z)\mathrm{d}z - \int_{\widehat{C}_+} f(n,z)\mathrm{d}z, \\ c_n^{(2b)} &= \int_{C_+} g(n,z)\mathrm{d}z = \int_{\widehat{C}_+} g(n,z)\mathrm{d}z, \end{aligned} \tag{13}$$

where use has been made of $\lim\limits_{z\to\infty} zf(n,z) = 0$ and $\lim\limits_{z\to\infty} zg(n,z) = 0$ for $0 \le \arg z < \pi/3$ or $2\pi/3 < \arg z \le \pi$.

3. ANALYTICAL EXPRESSION FOR OPTICAL FORCE

For the convenience of discussion, we still use the coordinate system x_c-o_c-y_c in the derivation of the optical force. For the region outside the dielectric cylinder $r > R$, the total field is a summation of the incident Airy beam field and the scattered field from the cylinder [25, 26], it can be written in form

$$E_z^{out}(r,\theta) = \sum_{n=-\infty}^{\infty} E_0 i^n \left[p_{1n}J_n(kr) + b_{1n}H_n^{(1)}(kr)\right] \exp(in\theta), \tag{14}$$

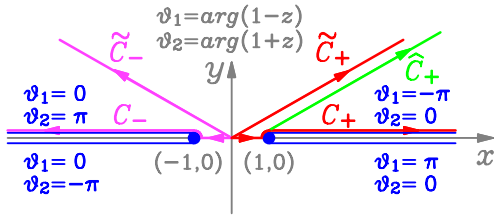

Figure 2. Schematic drawing of the contours C_- and C_+ for integration in Eq. (7). The alternative contours $\widetilde{C_-}$, $\widetilde{C_+}$, and $\widehat{C_+}$ in realistic numerical evaluation [Eq. (13)] are schematically shown as well.

where b_{1n} is the expansion coefficients of the scattered field and $H_n^{(1)}(kr)$ is the first kind Hankel function of the order n. As the dielectric cylinder is isotropic, the electric field inside the cylinder $r < R$ can be written as

$$E_z^{core}(r,\theta) = \sum_{-\infty}^{\infty} E_0 i^n d_{1n} J_n(k_c r) \exp(in\theta), \tag{15}$$

where d_{1n} is the expansion coefficients and k_c is the wave vector inside the cylinder. By using the the boundary conditions at the dielectric cylinder surface $r = R$, the Mie coefficients of the dielectric cylinder can be obtained

$$\begin{aligned} \frac{d_{1n}}{p_{1n}} &= \frac{k\mu_c \left[J_n(kR)H_n^{(1)\prime}(kR) - J_n'(kR)H_n^{(1)}(kR)\right]}{k\mu_c J_n(k_cR)H_n^{(1)\prime}(kR) - k_c\mu J_n'(k_cR)H_n^{(1)}(kR)}, \\ \frac{b_{1n}}{p_{1n}} &= \frac{k_c\mu J_n(kR)J_n'(k_cR) - k\mu_c J_n'(kR)J_n(k_cR)}{k\mu_c J_n(k_cR)H_n^{(1)\prime}(kR) - k_c\mu J_n'(k_cR)H_n^{(1)}(kR)}, \end{aligned} \tag{16}$$

where μ and μ_c are the permeabilities of the background medium and the the dielectric cylinder, respectively. For the case considered in present work, the nonmagnetic medium is considered so that $\mu = \mu_c = 1$. The superscript "$\prime$" in J_n' and $H_n^{(1)\prime}$ denotes the derivative of the Bessel function and the first kind Hankel function with respect to the argument. For a given Airy beam, the expansion coefficients p_{1n} can be easily determined by Eq. (7), and then the expansion coefficients d_{1n} and b_{1n} are uniquely determined according to Eq. (16). In this way, the electromagnetic field in the whole space can be obtained.

Now we turn to the calculation of the optical force imposed on the dielectric cylinder by an Airy beam. Starting from the time-averaged

Maxwell stress tensor [27]

$$\left\langle \bar{\bar{T}} \right\rangle = \frac{1}{2}\mathrm{Re}\left[\varepsilon_0\varepsilon \mathbf{E}\mathbf{E}^* + \mu_0\mu \mathbf{H}\mathbf{H}^* - \frac{1}{2}\left(\varepsilon_0\varepsilon \mathbf{E}\cdot\mathbf{E}^* + \mu_0\mu \mathbf{H}\cdot\mathbf{H}^*\right)\bar{\bar{I}}\right], \quad (17)$$

where $\bar{\bar{I}}$ is the unit tensor, ε_0 (ε) and μ_0 (μ) are the permittivity and permeability in the vacuum (background medium), respectively, and Re denotes the real part. $\mathbf{E} = E_z\hat{\mathbf{e}}_z$ is the total electric field, and $\mathbf{H} = H_{x_c}\hat{\mathbf{e}}_{x_c} + H_{y_c}\hat{\mathbf{e}}_{y_c} = H_r\hat{\mathbf{e}}_r + H_\theta\hat{\mathbf{e}}_\theta$ is the total magnetic field. For 2D case, the time-averaged electromagnetic force is

$$\mathbf{F} = \oint_L \left\langle \bar{\bar{T}} \right\rangle \cdot \hat{\mathbf{n}}\mathrm{d}l, \quad (18)$$

where $\hat{\mathbf{n}}$ is the outward unit normal vector, and $\mathrm{d}l$ is the length element of the integral curve L which can be chosen as any curve enclosing the dielectric cylinder if the background medium is lossless with real ε and μ. We choose an integral circle with radius r ($r > R$), and then the time-averaged force is

$$\mathbf{F} = \int_0^{2\pi} \left\langle \bar{\bar{T}} \right\rangle \cdot \hat{\mathbf{e}}_r r\mathrm{d}\theta, \quad (19)$$

where $\hat{\mathbf{e}}_r$ is the unit radial vector.

By using the asymptotic behavior of the Bessel function, the first kind Hankel function, and their first derivatives, we can obtain analytically the time-averaged force according to Eq. (19). The components are in form

$$\begin{aligned} F_x &= \mathrm{Re}[\mathcal{F}], \\ F_y &= \mathrm{Im}[\mathcal{F}], \\ F_z &= 0, \end{aligned} \quad (20)$$

where

$$\mathcal{F} = -\frac{\varepsilon_0\varepsilon}{k}\left[p^*_{1,n}b_{1,n-1} + p_{1,n-1}b^*_{1,n} + 2b_{1,n}b^*_{1,n+1}\right]. \quad (21)$$

$F_z = 0$ implies that the dielectric cylindrical particle experiences no optical force along z-axis due to the perpendicular incidence of the Airy beam. In the derivation of Eqs. (20)–(21), we have considered the the fact that the integral $\int_0^{2\pi} \begin{matrix}\cos\theta \\ \sin\theta\end{matrix} \mathrm{d}\theta$ makes the double summation $\sum_{m=-\infty}^{\infty}\sum_{n=-\infty}^{\infty}$ zero unless $m = n \pm 1$. In addition, for n runs from $-\infty$ to $+\infty$, we also have $\sum_n p_{1,n+1}b^*_{1,n} = \sum_n p_{1,n}b^*_{1,n-1}$. It is evident from Eq. (20)–(21) that the optical force is independent of the integral curve r due to the lossless characteristic of the ambient considered in our situation.

The local optical ray of the Airy beam is a parabolic curve, and the slope of the ray is $x/2k^2y_0^3$ when the parameter $\alpha = 0$. For the case when $\alpha \neq 0$, the slope is close to $x/2k^2y_0^3$ provided that α is very small [4, 18]. The intensity maxima of the Airy beam is a parabolic trajectory characterized by

$$y \cong \frac{1}{4}\frac{x^2}{k^2y_0^3} - 0.937173y_0, \tag{22}$$

where $0.937173y_0$ is the distance of the intensity maxima away from x-axis. Along the parabolic trajectory of the Airy beam particles can be accelerated, and the corresponding transverse acceleration of the Airy beam is $x^2/4k^2y_0^3$ [4, 10]. The optical force along the tangent and the normal direction of the parabolic intensity maxima read

$$\begin{aligned} F_t &= F_x\cos\beta + F_y\sin\beta, \\ F_n &= F_x\sin\beta - F_y\cos\beta, \end{aligned} \tag{23}$$

with $\tan\beta = x/2k^2y_0^3$ being the slope of the parabolic trajectory, as shown in Fig. 1.

It should be noted that with the increase of the parameter y_0 the width of the main lobe becomes larger and larger, meanwhile, the slope of the parabolic trajectory becomes lower and lower. When y_0 tends to infinity, the field in the main lobe of the Airy beam will be reduced to a plane wave propagating along x direction. The amplitude of this quasi-plane wave is $E_0\mathrm{Ai}(\Delta y/y_0)\exp(\alpha\Delta y/y_0)$ with $\Delta y = -0.937173y_0$. By taking $E_0 = \frac{1}{\mathrm{Ai}(\Delta y/y_0)\exp(\alpha\Delta y/y_0)}$, we have calculated the optical force imposed on a cylindrical particle placed in the center of the main lobe. As can be expected, the optical force in such case is the same as that imposed by a plane wave of unit amplitude [28]. This result can be served as an evidence that our method is correct and effective.

4. RESULTS AND DISCUSSION

For a particle placed in the Airy beam, an optical force will exert on it. At the same time, the particle also has effect on the field pattern of the Airy beam as shown in Fig. 3. Interestingly, the non-diffractive and self-healing properties [29] of the Airy beam can be observed. The Airy beam used in Fig. 3 has the wavelength $\lambda = 460\,\mathrm{nm}$, $y_0 = 4\lambda = 1.84\,\mu\mathrm{m}$, $\alpha = 0.08$, and $E_0 = 1$, propagating in the air. The dielectric cylinder placed in the center of the main lobe of the Airy beam has the permittivity $\varepsilon = 2.59$ and the radius $R = \lambda/4 = 115\,\mathrm{nm}$. The location of the dielectric cylinder is $(x_{c0}, y_{c0}) = (4.6\,\mu\mathrm{m}, -1.72\mu\mathrm{m})$ with y_{c0} determined according to Eq. (22). It can be seen from the

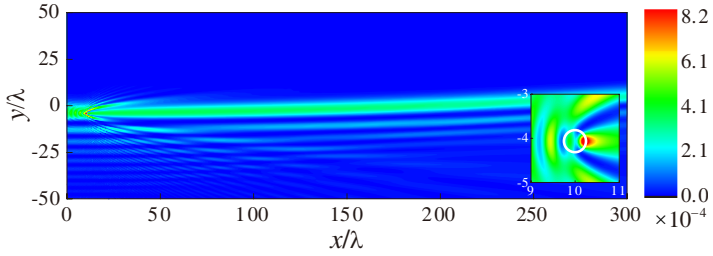

Figure 3. The field intensity pattern $|E_z|^2$ of the Airy beam scattered by a dielectric cylindrical particle. It is denoted by a white circle as can be seen from the inset where the amplified view of the field intensity pattern around the cylinder is presented.

inset that, locally, the Airy beam is remarkably disturbed. However, it recovers itself back after a finite distance.

To examine the acceleration property of a cylindrical particle by the Airy beam, we have calculated the optical force for the particle at different positions of the main lobe. The considered positions (x_{c0}, y_{c0}) are sampled uniformly in the center of the main lobe along the parabolic trajectory, satisfied by Eq. (22). They are also schematically illustrated in the inset of Fig. 4 where we present the tangent and the normal optical forces as the functions of the abscissa x_{c0} of the particle positions. They are calculated according to Eq. (23) and the parameters used are the same as those in Fig. 3. It is evident that the normal optical force is near zero, suggesting the frozen of the particle transverse to the parabolic curve, while a finite value of the tangent optical force indicates the acceleration of the particle along the parabolic curve. In addition, it can also be seen from Fig. 4 that the tangent optical force is slowly decreased in the long range of the parabolic curve, demonstrating the possibility to realize the long distance particle transport.

For a cylindrical particle placed off the center of the main lobe, it will lose the balance along the y direction. In Fig. 5, we have shown the x and y components of the optical force imposed on the particle versus its y coordinate. In the inset of Fig. 5, we also show schematically the particle positions. The tangent direction of the parabolic trajectory is nearly parallel to the x-axis, corresponding to the slope of about 0.002 at $x = 4.6\,\mu$m. At the center of the intensity maxima, the y component of the optical force is approximately zero, corresponding to the equilibrium position. If the particle is deviated away from this position, a y-component optical force will be exerted on the cylindrical particle, pulling it back as illustrated by the red dashed

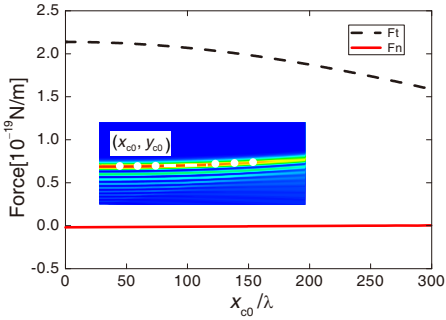

Figure 4. The tangent and the normal forces versus the abscissa x_{c0} of the dielectric cylindrical particle positions, which are denoted by the white dots and uniformly sampled along the center of the main lobe. The parameters are $\lambda = 460\,\text{nm}$, $y_0 = 4\lambda = 1.84\,\mu\text{m}$, $\alpha = 0.08$, $E_0 = 1$, $\varepsilon = 2.59$, and $R = \lambda/4 = 115\,\text{nm}$.

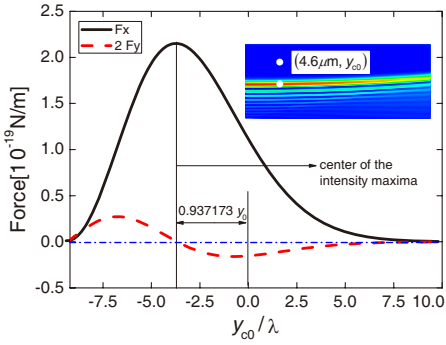

Figure 5. The x and y components of the optical force plotted as a function of the vertical coordinate y_{c0} of the particle position. The inset shows schematically the particle positions $(4.6\,\mu\text{m}, y_{c0})$ as denoted by the white dots. The parameters used are $\lambda = 460\,\text{nm}$, $y_0 = 4\lambda = 1.84\,\mu\text{m}$, $\alpha = 0.08$, $E_0 = 1$, $\varepsilon = 2.59$, and $R = \lambda/4 = 115\,\text{nm}$.

line in Fig. 5. The left and right zero points of the y component optical force correspond to the edge of the main lobe. The x component of the optical force is also shown in Fig. 5 as indicated by the black solid line. It can be seen that at the main lobe center of the Airy beam the x component of the optical force is the largest. At the edge of the main lobe, it also equal to zero as well. Accordingly, the particle can be accelerated along the parabolic trajectory of the main lobe of an Airy beam.

Our simulation also indicates that the trajectory for the particle acceleration depends on the size of the cylindrical particle. In Fig. 6, we present the positions at which zero normal optical force ($F_n = 0$) are imposed on the cylindrical particle of different radii R in the main lobe. At the positions given in Fig. 6, the tangent optical force exerted on the particle is positive and maximal. Accordingly, these positions correspond to the accelerating trajectory of the particles with different radii. As a reference, we also present the parabolic curve of the main lobe that is characterized by Eq. (22). It can be seen that for a very small particle, the accelerating trajectory coincides with the parabolic curve. With the increase of the particle size, the accelerating trajectory will deviate away from the parabolic curve. However, the particle can still be accelerated by the Airy beam along a nearly parabolic curve over long distance.

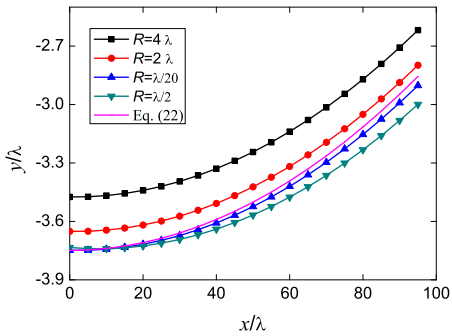

Figure 6. The positions correspond to the zero normal force ($F_n = 0$) in the main lobe of Airy beam for dielectric cylindrical particles of different radii R. The parameters used in the numerical calculations are $\lambda = 460\,\text{nm}$, $y_0 = 4\lambda = 1.84\,\mu\text{m}$, $\alpha = 0.08$, $E_0 = 1$, and $\varepsilon = 2.59$.

5. CONCLUSION

We have developed a rigorous full wave solution for the calculation of the optical force imposed on a cylindrical particle by an Airy beam. The non-diffractive and self-healing property of an Airy beam from the disturbance of a dielectric cylindrical particle is demonstrated in our simulation. The calculation of the optical force indicates that transverse to the parabolic curve of the main lobe of the Airy beam a cylindrical particle can be trapped, while along the parabolic curve of an Airy beam a finite optical force will be exerted on it, suggesting the capability of an Airy beam in accelerating the particle. At last, we have also examined the dependence of the effect on the size of the cylindrical

particle, which suggests that although the accelerating trajectories are a little different the long distance particle transport is still operable.

ACKNOWLEDGMENT

This work is supported by NNSFC (10774028 and 10904020) and MOE of China (B06011).

REFERENCES

1. Berry, M. V. and N. L. Balazs, "Nonspreading wave packets," *Am. J. Phys.*, Vol. 47, 264–267, 1979.
2. Unnikrishnan, K. and A. R. P. Rau, "Uniqueness of the Airy packet in quantum mechanics," *Am. J. Phys.*, Vol. 64, 1034–1035, 1996.
3. Siviloglou, G. A. and D. N. Christodoulides, "Accelerating finite energy Airy beams," *Opt. Lett.*, Vol. 32, 979–981, 2007.
4. Siviloglou, G. A., J. Broky, A. Dogariu, and D. N. Christodoulides, "Observation of accelerating airy beams," *Phys. Rev. Lett.*, Vol. 99, 213901, 2007.
5. Durnin, J., "Exact solutions for nondiffracting beams. I. The scalar theory," *J. Opt. Soc. Am. A*, Vol. 4, 651–654, 1987.
6. Durnin, J., J. J. Miceli, and J. H. Eberly, "Diffraction-free beams," *Phys. Rev. Lett.*, Vol. 58, 1499–1501, 1987.
7. Gutiérrez-Vega, J. C., M. D. Iturbe-Castillo, and S. Chávez-Cerda, "Alternative formulation for invariant optical fields: Mathieu beams," *Opt. Lett.*, Vol. 25, 1493–1495, 2000.
8. McGloin, D. and K. Dholakia, "Bessel Beams: Diffraction in a new light," *Contemp. Phys.*, Vol. 46, 15–28, 2005.
9. Turunen, J. and A. T. Friberg, *Progress of Optics*, Elsevier, Amsterdam, 2009.
10. Baumgartl, J., M. Mazilu, and K. Dholakia, "Optically mediated particle clearing using Airy wavepackets," *Nature Photonics*, Vol. 2, 675–678, 2008.
11. Ashkin, A., "Acceleration and trapping of particles by radiation pressure," *Phys. Rev. Lett.*, Vol. 24, 156–159, 1970.
12. Ashkin, A., J. M. Dziedzic, J. E. Bjorkholm, and S. Chu, "Observation of a single-beam gradient force optical trap for dielectric particles," *Opt. Lett.*, Vol. 11, 288–290, 1986.
13. Ashkin, A., *Optical Trapping and Manipulation of Neutral Particles Using Lasers*, World Scientific, Singapore, 2006.

14. Shiri, A. and A. Shoulaie, "A new methodology for magnetic force calculations between planar spiral coils," *Progress In Electromagnetics Research*, Vol. 95, 39–57, 2009.
15. Ravaud, R., G. Lemarquand, V. Lemarquand, S. Babic, and C. Akyel, "Mutual inductance and force exerted between thick coils," *Progress In Electromagnetics Research*, Vol. 102, 367–380, 2010.
16. Garces-Chavez, V., D. McGloin, H. Melville, W. Sibbett, and K. Dholakia, "Simultaneous micromanipulation in multiple planes using a self-reconstructing light beam," *Nature*, Vol. 419, 145–147, 2002.
17. Ng, J., Z. F. Lin, and C. T. Chan, "Theory of optical trapping by an optical vortex beam," *Phys. Rev. Lett.*, Vol. 104, 103601, 2010.
18. Besieris, I. M. and A. M. Shaarawi, "A note on an accelerating finite energy Airy beam," *Opt. Lett.*, Vol. 32, 2447–2449, 2007.
19. Siviloglou, G. A., J. Broky, A. Dogariu, and D. N. Christodoulides, "Ballistic dynamics of Airy beams," *Opt. Lett.*, Vol. 33, 207–209, 2008.
20. Novitsky, A. V. and D. V. Novitsky, "Nonparaxial Airy beams: role of evanescent waves," *Opt. Lett.*, Vol. 34, 3430–3432, 2009.
21. Novotny, L. and B. Hecht, *Principles of Nano-optics*, Cambridge University Press, Cambridge, 2006.
22. Mahillo-Isla, R., M. J. González-Morales, and C. Dehesa-Martínez, "Plane wave spectrum of 2D complex beams," *Journal of Electromagnetic Waves and Applications*, Vol. 23, No. 8–9, 1123–1131, 2009.
23. Vallée, O. and M. Soares, *Airy Functions and Applications to Physics*, World Scientific, Singapore, 2004.
24. Lim, W.-G. and J.-W. Yu, "Scattering by a dielectric-loaded conducting wedgge with concaved dege: TE case," *Progress In Electromagnetics Research*, Vol. 89, 85–100, 2009.
25. Sun, X. M., H. H. Wang, and H. Y. Zhang, "Scattering by an infinite cylinder arbitrarily illuminated with a couple of Gaussian beams," *Journal of Electromagnetic Waves and Applications*, Vol. 24, No. 10, 1329–1339, 2010.
26. Li, H.-Y., Z.-S. Wu, and L. Bai, "Scattering for charged multisphere structure located in plane wave/Gaussian beam," *Journal of Electromagnetic Waves and Applications*, Vol. 24, No. 14–15, 2037–2047, 2010.
27. Jackson, J. D., *Classical Electrodynamics*, 3rd edition, 2004.
28. Grzegorczyk, T. M. and J. A. Kong, "Analytical expression of the

force due to multiple TM plane-wave inciddences on an infinite lossless dieletric circular cylinder of arbitrary size," *J. Opt. Soc. Am. B*, Vol. 24, 644–652, 2007.

29. Broky, J., G. A. Siviloglou, A. Dogariu, and D. N. Christodoulides, "Self-healing properties of optical Airy beams," *Opt. Express*, Vol. 16, 12880–12891, 2008.